Supporting Information

Hydrogen bond enhanced coordination of hydrogen peroxide to indium trichloride

Nikita S. Mayorov,[a] Pavel A. Egorov,[a] Alexander G. Medvedev,[a], Evgeny S. Belyaev,[b] Oleg A. Filippov,[c] Natalia V. Belkova,[c] Alexey A. Mikhaylov,[a] Maxim N. Sokolov,[d] Ovadia Lev*[e] and Petr V. Prikhodchenko*[a]*

[a.] N.S. Kurnakov Institute of General and Inorganic Chemistry, Russian Academy of Sciences, Leninskii pr. 31, Moscow 119991, Russian Federation; prikhman@gmail.com.

[b.] Frumkin Institute of Physical Chemistry and Electrochemistry of the Russian Academy of Sciences, Leninskii pr. 31-4, Moscow 119071, Russian Federation

[c.] A.N. Nesmeyanov Institute of Organoelement Compounds, Russian Academy of Sciences, Vavilov Str. 28, Moscow 119334, Russian Federation; nataliabelk@ineos.ac.ru

[d.] Nikolaev Institute of Inorganic Chemistry, Siberian Branch of the Russian Academy of Sciences, prosp. Academika Lavrentieva 3, 630090 Novosibirsk, Russian Federation.

[e.] Casali Center of Applied Chemistry, Hebrew University of Jerusalem, Jerusalem 9190401, Israel; ovadia@mail.huji.ac.il

Table of contents

1. MATERIALS AND METHODS

1.1. Materials

$InCl_3$ (99.999 wt.%) was purchased from Lanhit (Russia) and used without further purification. Et_2O and hydrogen peroxide (30 wt.%) were purchased from Aldosa (Russia). Et_2O was dried over molecular sieves (3 Å) and freshly distilled prior to use. To obtain nearly anhydrous solvents, molecular sieves were replaced several times before using the solvent. 18-crown-6 ether (>99.0%) was purchased from Macklin (China), dried by slow azeotropic evaporation with hexane, and subsequently stored over P_2O_5 until completely dry. 15-crown-5 ether (>97.0%) was purchased from ChemicalLine (Russia) and stored over P_2O_5 until completely dry.

Glassware for peroxide-rich solutions: All glassware was treated by filling with 1M NaOH for 1 day, then with 1M nitric acid for an additional day, and finally with 10 wt.% hydrogen peroxide for another day. Dichromate or permanganate treatment should be avoided.

Purification of H_2O_2.

Commercial hydrogen peroxide was concentrated by vacuum distillation. First, 30 wt% hydrogen peroxide was distilled under vacuum to remove stabilizers and other impurities. Thus obtained 10 wt% pure aqueous hydrogen peroxide was concentrated by rectification under vacuum and controlled boiling by passing argon resulting in 99.9 wt% hydrogen peroxide as determined by permanganometry.[1,2]

Safety note: Concentrating hydrogen peroxide solutions and working with them requires safety precautions. Handling procedures for concentrated hydrogen peroxide are described in detail (danger of explosion!).[1]

CAUTION! Storage of concentrated hydrogen peroxide systems in a closed container is strictly prohibited due to safety concerns.

1.2. Synthesis

All manipulations for the synthesis of compounds **1**-**5** were performed in an argon-filled glovebox. Dispersions and solutions containing hydrogen peroxide were loosely sealed with a polyethylene stopper to prevent pressure build-up in the system due to possible decomposition of hydrogen peroxide due to safety concerns.

*Synthesis of $[InCl_2(15\text{-crown-}5)]^+[InCl_4]^-$ (**1**)*

$InCl_3$ (0.050 g, 0.226 mmol) was suspended in 99.9% H_2O_2 (0.077 g, 2.261 mmol). Slow bubble evolution was observed during stirring. Subsequently, 15-crown-5-ether (0.050 g, 0.227 mmol) was carefully added to the reaction mixture and stirred for 10 min. Partial dissolution of the initial $InCl_3$ was observed. The vial with resulting dispersion was loosely sealed by a polyethylene stopper, placed in a desiccator over P_2O_5, and maintained in a refrigerator at -20°C overnight. Colorless uniform crystals were obtained.

Compound **1** is unstable in atmospheric moisture. X-ray diffractograms recorded from a polycrystalline sample of complex **1** were compared with the diffractogram simulated from the single crystal X-ray diffraction data (Fig. S1).

*Synthesis of $[mer\text{-}InCl_3(H_2O_2)(H_2O)_2]\cdot$18-crown-6 (**2**)*

$InCl_3$ (0.050 g, 0.226 mmol) was suspended in 99.9% H_2O_2 (0.077 g, 2.261 mmol). Slow bubble evolution was observed during stirring. Subsequently, the solution of 18-crown-6-ether (0.060 g, 0.227 mmol) in 99.9% H_2O_2 (0.039 g, 1.131 mmol) was carefully added and stirred for 10 min. Partial dissolution of the initial $InCl_3$ was observed. The vial with resulting dispersion was loosely sealed by a polyethylene stopper, placed in a desiccator over P_2O_5, and maintained in a refrigerator at -20°C overnight. Colorless uniform crystals were obtained.

*Alternative synthesis of compound **2**.*

Compound **3** (0.030 g, 0.062 mmol) was suspended in 95.0% H_2O_2 (0.300 g, 8.379 mmol) and mixed for 5 min by shaking. Complete dissolution of the initial complex was observed. The vial with the resulting solution was loosely sealed by a polyethylene stopper, placed in a desiccator over P_2O_5, and maintained in a refrigerator at -20°C overnight. Colorless uniform crystals were obtained.

*Alternative synthesis of compound **2**.*

$InCl_3$ (0.030 g, 0.136 mmol) was dissolved in 4 mL of Et_2O. Subsequently, 0.5 mL of combined solution of 18-crown-6 (0.274 M, 0.137 mmol) and 95.0% H_2O_2 (5.44 M, 2.720 mmol) in Et_2O was added dropwise. During the addition of the crown ether and hydrogen peroxide solution, precipitation was observed. The vial was loosely sealed by a polyethylene stopper and placed in a desiccator over P_2O_5 and maintained in a refrigerator at -20 °C.

The compound **2** is unstable at ambient conditions and converts into the [*mer*-$InCl_3(H_2O)_3]\cdot$18-crown-6 complex (Fig. S4).[3]

X-ray diffractograms recorded from a polycrystalline sample of complex **2** were compared with the diffractogram simulated from the single crystal X-ray diffraction data (Fig. S5).

*Synthesis of [fac-$InCl_3$(18-crown-6)] (**3**)*

$InCl_3$ (0.100 g, 0.452 mmol) was dissolved in 15 mL of Et_2O. Then 5 ml of 0.1 M solution of 18-crown-6 (0.500 mmol) was added dropwise to the solution of $InCl_3$. The resulting mixture was stirred for 3 h. After standing without stirring for 30 min, the solid was collected by vacuum filtration using a glass funnel filter. The colorless uniform crystals were washed with diethyl ether (5 mL) Yield 98.9% (0.217 g).

Anal. Calc. for $C_{12}H_{24}Cl_3O_6In$ (**3**): C, 29.69; H, 4.98. Found: C, 25.33; H, 3.92.

*Alternative synthesisof compound **3**.*

$InCl_3$ (0.100 g, 0.452 mmol) was added to a 20 mL of 0.025 M solution of 18-crown-6 (0.500 mmol). The resulting mixture was stirred for 3 h. After standing without stirring for 30 min, the solid was collected by vacuum filtration using a glass funnel filter. The colorless uniform crystals were washed with diethyl ether (5 mL). The experimental powder X-ray diffractogram of **3** obtained in an inert perfluorinated oil at 298K fitted with the diffractogram simulated from the single crystal X-ray diffraction data (Fig. S10).

*Synthesis of $[InCl_2(18\text{-crown-}6)]^+[InCl_4(H_2O_2)]^-$ (**4**)*

Compound **3** (0.030 g, 0.062 mmol) was suspended in 99.9% H_2O_2 (0.500 g, 14.685 mmol) and mixed for 15 min by shaking. Complete dissolution of the initial complex was observed. The vial with the resulting solution was loosely sealed by a polyethylene stopper, placed in a desiccator over P_2O_5, and maintained in a refrigerator at -20°C overnight. Colorless uniform crystals were obtained.

The compound is unstable at ambient conditions. X-ray diffractograms recorded from a polycrystalline sample of complex **4** were compared with the diffractogram simulated from the single crystal X-ray diffraction data (Fig. S11).

*Reaction of complex **4** with water* as *a 95% H_2O_2*:

10 equivalents of water (0.62 mmol per In(III)) were added to the crystals of complex **4** in the mother liquor as a 95% H_2O_2 (0.224 g). The vial with resulting solution was loosely sealed by a polyethylene stopper, placed in a desiccator over P_2O_5, and maintained in a refrigerator at -20°C overnight. Colorless uniform crystals of complex **2** were obtained (Fig. S13).

*Reaction of complex **4** with water as a 0.2 M solution in Et_2O*:

5 equivalents of water (0.31 mmol per In(III)) were added to the crystals of complex **4** in the mother liquor as 1.55 mL of a 0.2 M H_2O solution in Et_2O. The vial with resulting solution was loosely sealed by a polyethylene stopper, placed in a desiccator over P_2O_5, and maintained in a refrigerator at -20°C overnight. Colorless uniform crystals of [*mer*-$InCl_3(H_2O)_3$]·18-crown-6 were obtained (Fig. S14).

*Synthesis of $[InCl_3(H_2O)_{0.5}(H_2O_2)_{0.5}$(18-Crown-6)] (**5**):*

$InCl_3$ (0.030 g, 0.136 mmol) was dissolved in 25 mL of Et_2O. Subsequently, 1 mL of a combined solution of 18-crown-6 (0.137 M, 0.137 mmol) and 99.9% H_2O_2 (6.791 M, 6.791 mmol) in Et_2O was added dropwise. During the addition of the crown ether and hydrogen peroxide solution, precipitation was observed. The vial was loosely sealed by a polyethylene stopper and placed in a desiccator over P_2O_5 and maintained in a refrigerator at -20 ºC. Crystals suitable for X-ray diffraction analysis formed within 1–2 days.

*Alternative synthesis of compound **5**.*

Compound **3** (0.030 g, 0.062 mmol) was added to a 10 mL of 0.31 M solution of 99.9% H_2O_2 (3.087 mmol) in Et_2O. The vial with resulting dispersion was loosely sealed by a polyethylene stopper, placed in a desiccator over P_2O_5, and maintained in a refrigerator at -20°C overnight.

Compound **5** is unstable at ambient conditions. X-ray diffractograms recorded from a polycrystalline sample of complex **5** were compared with the diffractogram simulated from the single crystal X-ray diffraction data (Fig. S16).

Synthesis of [mer-$InCl_3(H_2O)_3$]·18-crown-6:

$InCl_3$ (0.044 g, 0.20 mmol) was dissolved in 5 mL of Et_2O. Then, 1 mL of a 0.2 M solution of 18-crown-6 in Et_2O (0.20 mmol) was added. Subsequently 3 mL of a 0.2 M solution of H_2O in Et_2O, (0.60 mmol) was added, and the mixture was stirred overnight. The resulting precipitate was filtered and washed with Et_2O and dried in a vacuum desiccator. Yield: 0.113 g (94.6%).

The experimental powder X-ray diffractogram of [*mer*-$InCl_3(H_2O)_3$]·18-crown-6 was compared with simulated from the single crystal X-ray diffraction data (Fig. S7)[3].

Preparation of solutions for NMR studies

All solutions were prepared in an argon-filled glovebox. For the ^{1}H NMR experiments, a 0.2 M solution of H_2O_2 and a 0.05 M solution of $InCl_3$ in Et_2O were initially prepared and subsequently used to obtain 0.03 M solution of H_2O_2 in Et_2O and 0.03 M solution of the equimolar mixture of $InCl_3$ and H_2O_2 in Et_2O.

Preparation of 0.2 M H_2O_2 solution in Et_2O: 99.9 wt.% H_2O_2 (0.068 g, 2 mmol) was added to 10 ml volumetric flask, and the volume was brought to the mark with Et_2O.

Preparation of 0.05 M $InCl_3$ solution in Et_2O: $InCl_3$ (0.055 g, 0.25 mmol) was dissolved in 5 ml volumetric flask, and the volume was brought to the mark with Et_2O.

*Preparation of a 0.03 M solution of H_2O_2 in Et_2O: 0.*15 ml of 0.2 M H_2O_2 solution in Et_2O was added to 0.85 ml of Et_2O.

Preparation of a 0.03 M solution of the equimolar mixture of $InCl_3$ and H_2O_2 in Et_2O: 0.15 ml of 0.2 M H_2O_2 solution in Et_2O was added to the 0.60 ml of 0.05 M $InCl_3$ solution in Et_2O. Then 0.25 ml of Et_2O was added.

Preparation of an Indium Standard Sample: $InCl_3$ (0.275 g 1.244 mmol) was dissolved in 1 ml of concentrated hydrochloric acid. The resulting solution was extracted with 5 ml of Et_2O.

Preparation of a solution $InCl_3$, 15-Crown-5 in H_2O_2: a) $InCl_3$ (0.050 g, 0.226 mmol) was added to a solution of 15-crown-5 (0.025 g, 0.113 mmol) in 0.7 ml of H_2O_2. The resulting suspension was filtered and the filtrate was transferred to an NMR tube.

b) $InCl_3$ (0.050 g, 0.226 mmol) was added to a solution of 15-crown-5 (0.025 g, 0.113 mmol) in 0.7 ml of H_2O_2. The resulting suspension was allowed to stand for one day in refrigerator, then filtered, and the filtrate was transferred to an NMR tube.

Preparation of a 0.3 M $InCl_3$ in an equimolar mixture of H_2O_2 and Et_2O: $InCl_3$ (0.050 g, 0.226 mmol) was dissolved in 0.7 ml of a H_2O_2/Et_2O (1:1 molar ratio).

1.3. Characterization

Elemental analysis. Carbon and hydrogen content were determined using the vario MICRO cube analyzer (Elementar, Germany).

X-ray powder diffraction measurements were performed on a D8 Advance diffractometer (Bruker AXS, Germany) with a goniometer radius of 280 mm. The crystals were isolated from the mother liquor with a glass spatula and subsequently dried using a glass-fiber filter. The obtained solid was mixed with perfluorinated Fomblin YR-1800 oil and loaded into

low-background quartz sample holders. XRD patterns in the range 5˚ to 30˚ 2θ were recorded at 298K using CuKα radiation (λ=1.5418 Å) under the following measurement conditions: tube voltage of 40 kV, tube current of 40 mA, step scan mode with a step size 0.02˚ 2θ, and counting time of 1 s/step. XRD patterns were processed by DiffracPlus software. Given that the obtained complexes are moisture-sensitive debye powder X-ray patterns for compounds **1**, **2**, **4**, **5** at 100K were obtained on a single-crystal diffractometer Bruker D8 Venture using Cu Kα radiation (λ = 1.5418 Å) at 100K. The operation temperature was controlled by a Cryostream 800 Plus device (Oxford Cryosystems). The Debye ring integration was processed in SAINT (V8.38A, Bruker) software. Sample preparation was carried out similarly to the preparation of samples for X-ray diffraction of single crystals, except that instead of a single crystal, finely ground crystals in perfluorinated oil were mounted on the goniometer head. Notably, the experimental patterns show a shift of all reflections relative to the simulated ones by the same 2θ value, likely due to slight variations in the thickness of the crystal layer on the goniometer head.

X-ray analysis. Single crystals of **1**-**5** suitable for X-ray analysis were collected from corresponding mother liquor without additional recrystallization placed on microscope slides, and then coated with a perfluorinated oil (Fomblin YR-1800). An OLYMPUS SZ61 polarizing microscope equipped with a Linkam PE-120 stage cooling attachment and a LINKAM T96-P controller was used for crystal collection at -12°C to prevent the decomposition of hydrogen peroxide complexes. Subsequently, appropriate single crystals were mounted on MicroMeshes™ (MiTeGen) and then immediately positioned beneath a cold stream of nitrogen. Experimental intensities were measured on a Bruker SMART APEX II and Bruker D8 Venture diffractometers (graphite monochromatized MoK_α radiation, λ = 0.71073 Å) using ω-scan mode at 100 K. Absorption corrections based on measurements of equivalent reflections were applied.[5] The gausian structures were solved by direct methods and refined by full-matrix least-squares on F^2 with anisotropic thermal parameters for all non-hydrogen atoms.[6] Hydrogen atoms of macrocyclic ether in **1**-**5** were placed in idealized positions and refined using a riding model. Hydrogen atoms of hydrogen peroxide and water ligands were found from difference Fourier synthesis and freely refined (**4**) or refined with distance restraint (**2**, **5**). In **1** and **3**, 15-crown-5 and 18-crown-6 molecules were found to be disordered over two positions with 0.5 / 0.5 and 0.626(8) / 0.374(8) occupancies ratio, respectively. In **5**, the ratio of isomorphous substitution H_2O_2 / H_2O equals 0.5 / 0.5. Compound **1** was refined as a 2-component inversion twin by the law (−1 0 0 0 -1 0 0 0 −1). X-ray diffraction studies were performed at the Centre of Shared Equipment of IGIC RAS. Selected crystallographic data for **1-5** are provided in Table S1.

Selected atom distances and bond angles are collected in Table S2. The crystallographic data for **1-5** have been deposited with the Cambridge Crystallographic Data Centre as supplementary publication under the CCDC numbers 2381797, 2355318, 2431050-2431053, respectively.

FTIR spectra were recorded on a JASCO FT/IR-4600 spectrometer. Spectra processing was performed using JASCO Spectra Manager software. The spectra were subjected to ATR correction, baseline offset correction, and smoothing. For complex **2**, IR spectra were acquired in vaseline oil (Nujol) rather than perfluorinated oil, (Fig. S6) since it doesn't have absorption bands in 1200-800 cm^{-1} which could overlap with absorption bands of compound.

Differential thermal analysis (DTA) and **thermogravimetry analysis** (TGA) were performed on simultaneous thermal analyzer, DTG-60 (Shimadzu). All experiments were carried out under argon flow at a heating rate of 10 °C/min.

The sample of complex **2** for thermal analysis was prepared in a glovebox under argon atmosphere by isolating the material from the reaction mixture and removing excess H_2O_2 from the crystal surface using glass-fiber filter. Upon heating, the DTA curve initially exhibits two endothermic effects with maxima at 63 °C and 87 °C, accompanied by mass loss, which can be attributed to the removal of water (Fig. S8). Further heating leads to the appearance of two exothermic peaks, also accompanied by mass loss. The first peak, with a maximum at 107 °C, can be attributed to residual free H_2O_2 remaining on the crystal surface due to incomplete removal of excess H_2O_2. A similar exothermic effect with a maximum at 108 °C is observed for the Al_2O_3 – H_2O_2 (5.6:1) system. The second exothermic peak, with a maximum at 126 °C, is most likely associated with the decomposition of complex **2**.

^{1}H and ^{115}In The NMR spectra (δ, ppm) were recorded on a Bruker AVANCE III 600 spectrometer operating at 600.13 MHz and 131.50 MHz respectively. The ^{1}H NMR spectra were recorded at 25 ºC, 0 ºC, −20 ºC and −40 ºC. The ^{115}In NMR spectra were recorded at 25 ºC. A sealed ampule containing $CDCl_3$ placed inside the NMR tube was used as an external standard. The ^{1}H NMR spectra were referenced to the residual $CHCl_3$ signal (7.26 ppm) in the $CDCl_3$. NMR spectra were processed by TopSpin software.

^{115}In NMR studies are limited due to the high nuclear spin of the ^{115}In atom (I = 9/2) and its large quadrupole moment, which leads to signal broadening when studying ions with symmetry lower than tetrahedral[7–9]. The exchange of solvent molecules with the solvation shell

of six-coordinate ions causes broadening of the spectral lines, which is why these complexes are often not observed in solutions.

An ^{115}In NMR spectrum of a standard sample revealed a resonance peak at 401 ppm (Fig. S18) which is presumably attributed to the anionic form $InCl_4^-$ (literature value: 440 ppm[9]).

Subsequently, we attempted to record ^{115}In NMR spectra from a freshly prepared solution of $InCl_3$ and 15-crown-5 (1/2 equiv) in hydrogen peroxide (Fig. S18) and from a similar solution that had stood for one day (Fig. S19). This was motivated by the fact that this is the only system in our work in which the tetrahedral $InCl_4^-$ anion has been obtained. It should be noted that, since complex **1** is slightly soluble in H_2O_2, a saturated solution was used for the NMR measurements. The resulting spectra lack distinct signals, which could be a consequence of the asymmetric coordination environment of the indium ion in the solution.

We also attempted to record ^{115}In NMR spectrum of the solution of indium chloride in Et_2O/H_2O_2 mixture (Et_2O/H_2O_2 = 1/1), but again, no distinct signals were observed (Fig. S19).

Thus, ^{115}In NMR spectroscopy is not suitable for studying the coordination of hydrogen peroxide with In(III) in the obtained $InCl_3$-H_2O_2-ether system, since it does not contain indium anions with spherical symmetry.

1.4. DFT calculations

DFT calculations were performed with the Gaussian 09[10] package at the DFT/ωB97XD level[11] without any ligand simplification. ω-B97xD is a range-separated hybrid functional that includes long-range corrections and empirical dispersion and typically accurately predicts bond lengths, angles, and interaction energies for hydrogen bond[12,13]. For all atoms, the Def2-TZVPP basis[14] set was applied, providing the necessary "larger space occupation" for hydrogen-bond-forming orbitals[15], and supplied with ECP[15] for In atoms. The structures of all complexes were fully optimized in water described by the CPCM model,[17,18] without any symmetry restrictions. The nature of all the stationary points on the potential energy surfaces was confirmed by vibrational analysis. Molecular electrostatic potential surfaces were generated by Gaussian 09 and further analyzed by the Multiwfn package.[19]

2. FIGURES

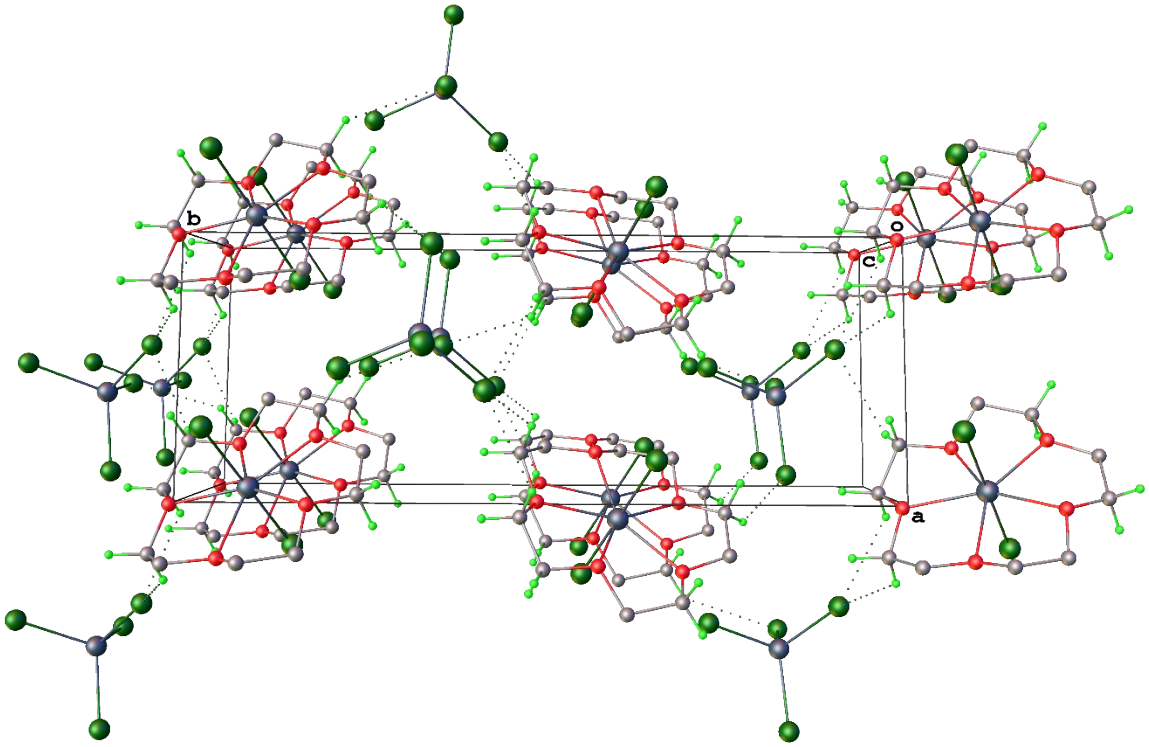

Figure S1. Packing in the crystal structure of **1**. Disordered fragments of 15-crown-5 ether are omitted for clarity**.**

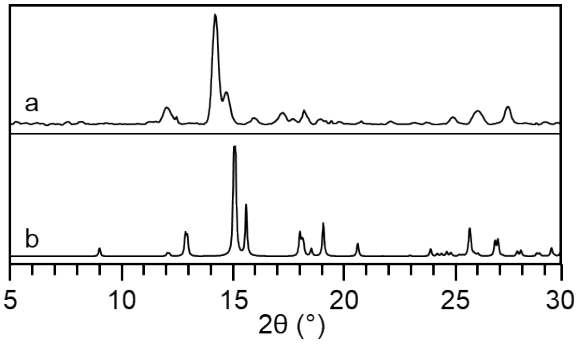

Figure S2. X-ray diffractograms recorded from a polycrystalline sample of complex **1** at 100 K on a single-crystal diffractometer (a) and simulated from corresponding scXRD data (b).

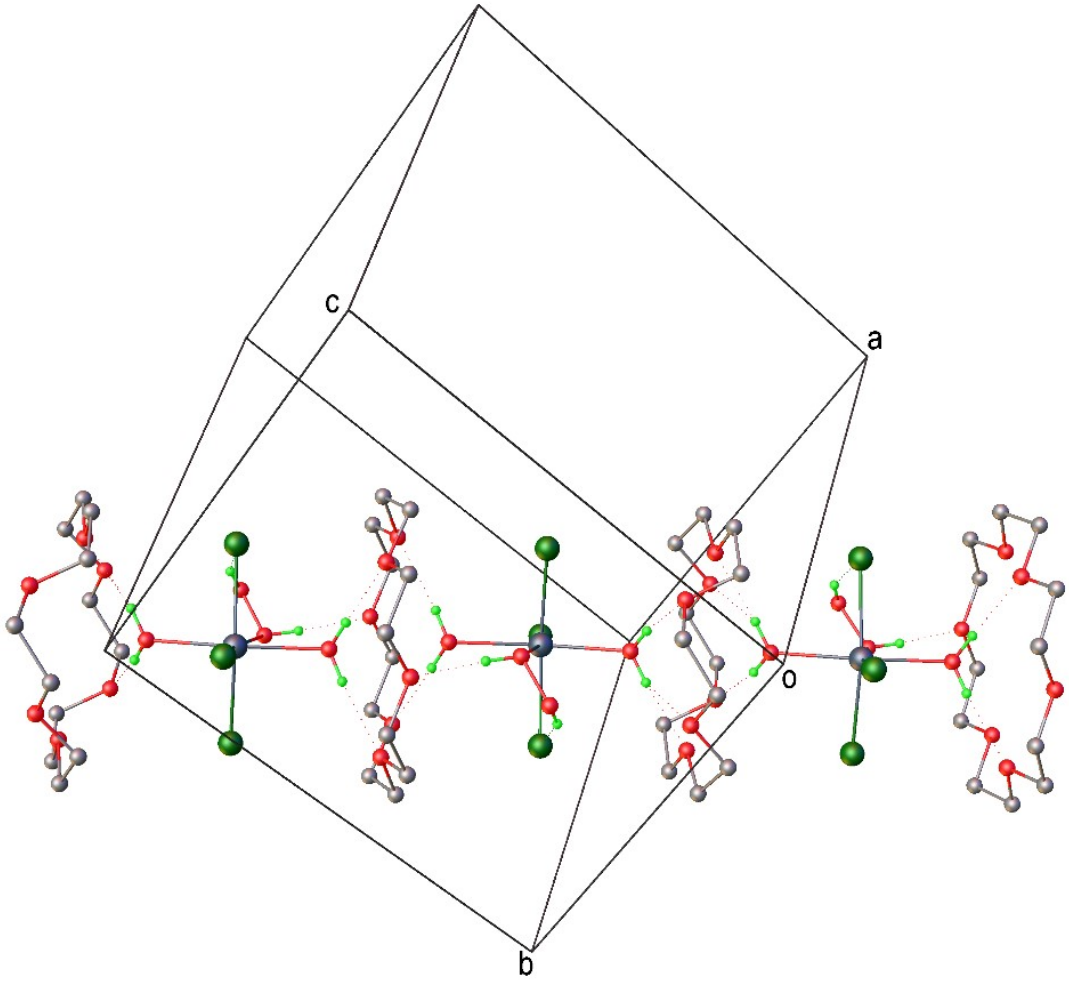

Figure S3. The chains in the crystal structure of **2**. H-bonds are shown by a dotted line. H-atoms of macrocyclic ether are omitted for clarity.

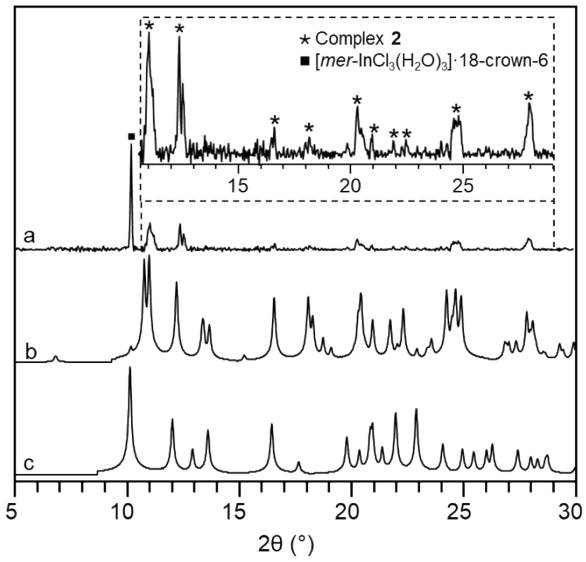

Figure S4. X-ray diffractograms recorded from a polycrystalline sample of complex **2** at 298K on a powder diffractometer (a) and simulated from corresponding scXRD data for [*mer*-$InCl_3(H_2O)_2(H_2O_2)$]·18-crown-6 (b) and [*mer*-$InCl_3(H_2O)_3$]·18-crown-6 (c).

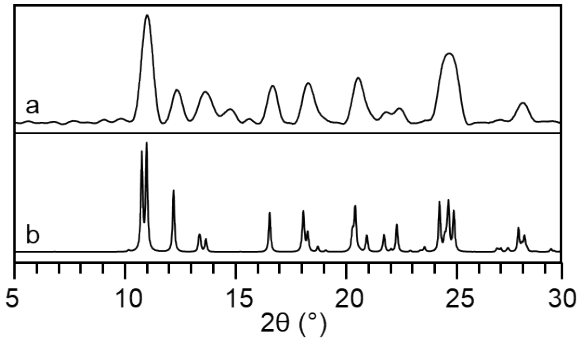

Figure S5. X-ray diffractograms recorded from a polycrystalline sample of complex **2** at 100 K on a single-crystal diffractometer (a) and simulated from corresponding scXRD data (b).

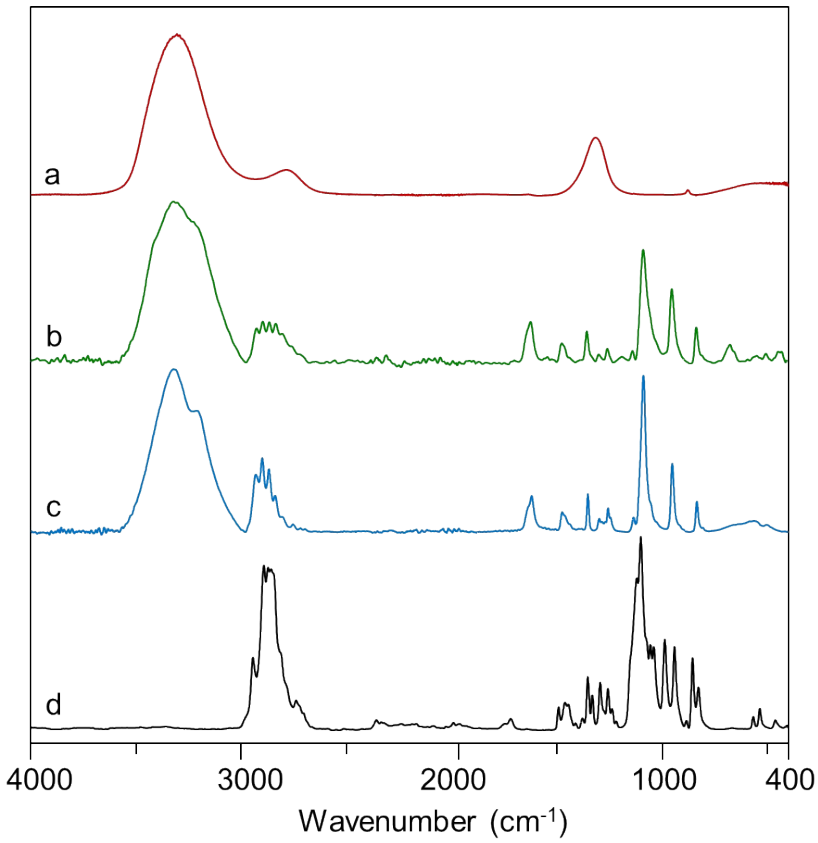

Figure S6. FTIR spectra of 99.9 wt% H_2O_2 (a), complex **2** in Vaseline oil (b), [*mer*-$InCl_3(H_2O)_3$]·18-crown-6 (c), and 18-crown-6 (d).

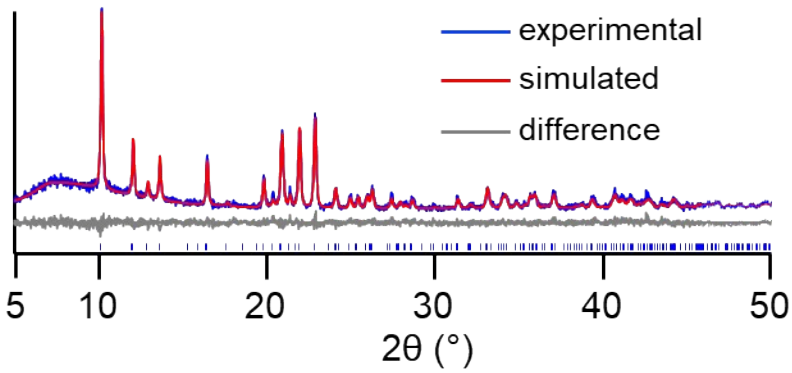

Figure S7. Fitting patterns of [*mer*-$InCl_3(H_2O)_3$]·18-crown-6. The experimental and simulated intensities are plotted as blue and red solid lines respectively. The gray line at the bottom is their intensity difference. The tick marks indicate the positions of all possible Bragg reflections from the structure model**.**

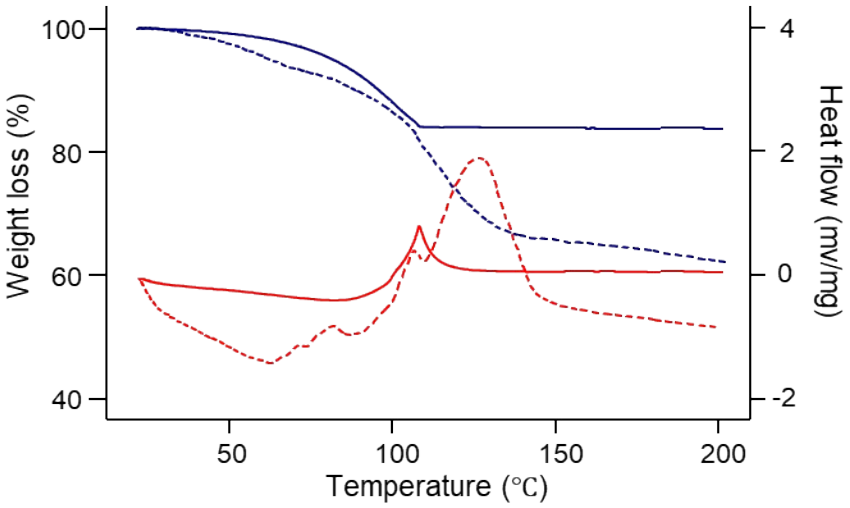

Figure S8. TGA (blue) and DTA (red) curves of complex **2** (dashed lines) and Al_2O_3 – H_2O_2 (5.6:1) mixture (solid lines)

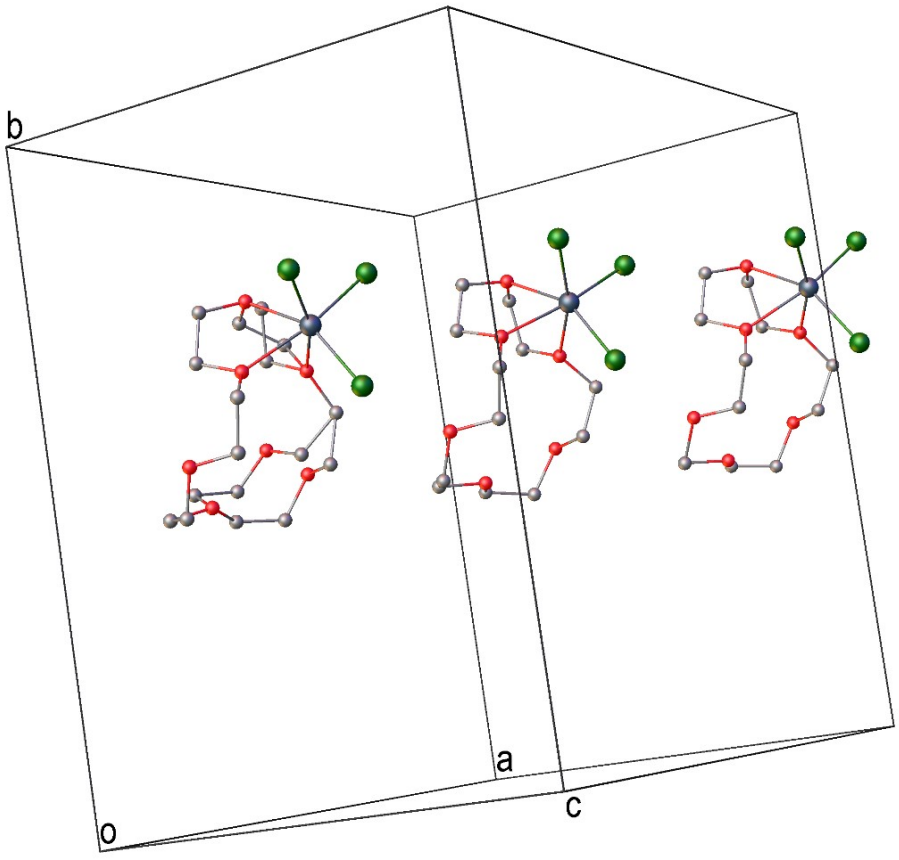

Figure S9. Asymmetric unit of the crystal structure of **3**. H-atoms of macrocyclic ether are omitted for clarity.

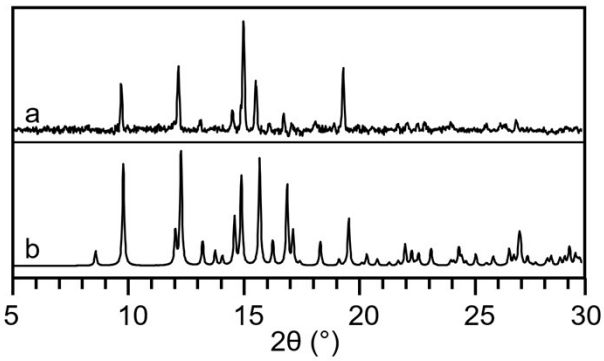

Figure S10. X-ray diffractograms recorded from a polycrystalline sample of complex **3** at 298K on a powder diffractometer (a) and simulated from corresponding scXRD data (b).

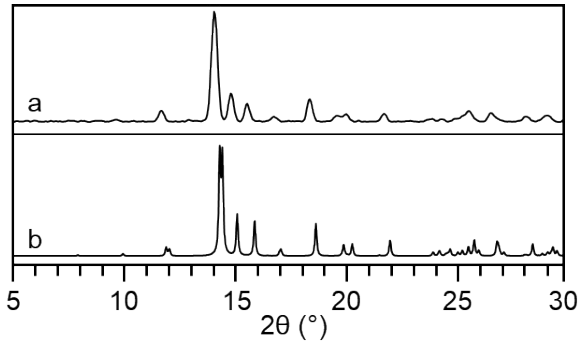

Figure S11. X-ray diffractograms recorded from a polycrystalline sample of complex **4** at 100 K on a single-crystal diffractometer (a) and simulated from corresponding scXRD data (b).

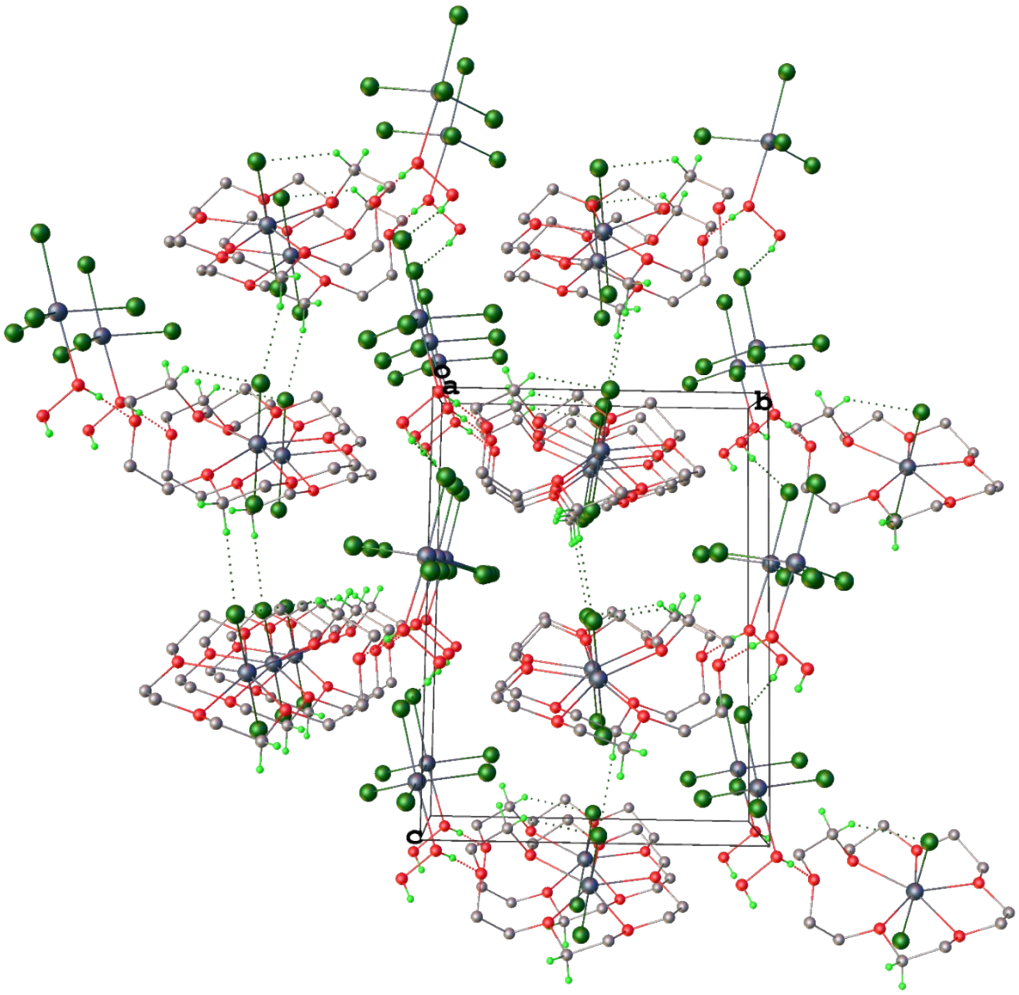

Figure S12. Packing in the crystal structure of **4**. H-atoms not involved in hydrogen bonding are omitted for clarity.

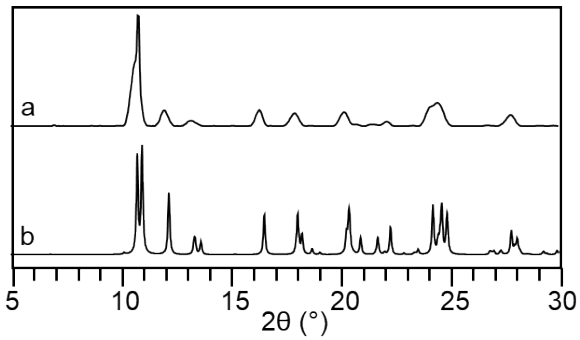

Figure S13. X-ray diffractograms recorded from a polycrystalline sample obtained at 100 K on a single-crystal diffractometer after addition of 10 equivalents of water as a 95% H_2O_2 to a complex **4** (a) and simulated from corresponding scXRD data for complex 2 (b).

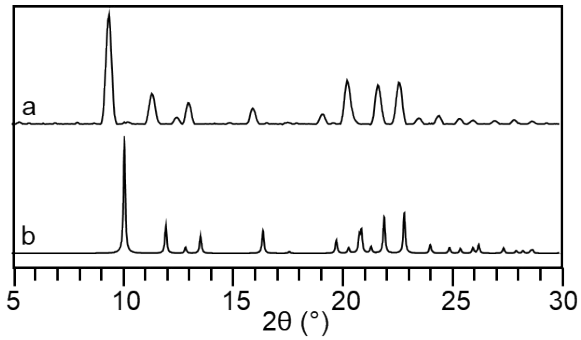

Figure S14. X-ray diffractograms recorded from a polycrystalline sample obtained at 100 K on a single-crystal diffractometer after addition of 5 equivalents of water in the form of a 0.2 M solution in diethyl ether to a complex **4** (a) and simulated from corresponding scXRD data for complex [*mer*-$InCl_3(H_2O)_3$]·18-crown-6 (b)

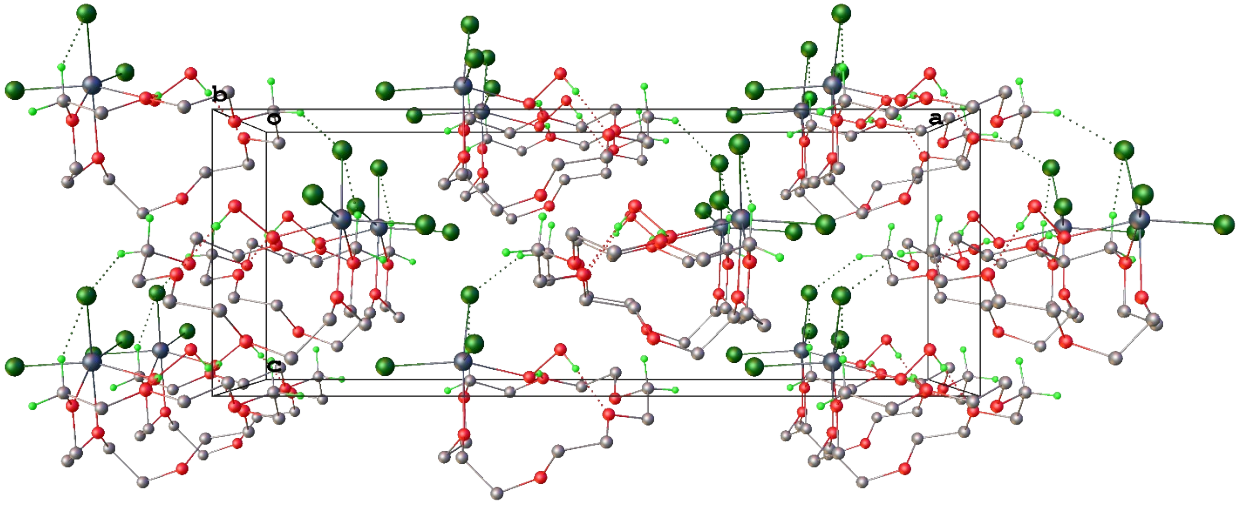

Figure S15. Packing in the crystal structure of **5**. H-atoms not involved in hydrogen bonding and coordinated water molecules are omitted for clarity.

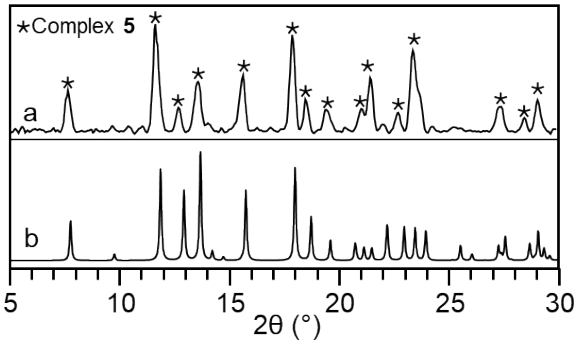

Figure S16. X-ray diffractograms recorded from a polycrystalline sample of complex **5** at 100 K on a single-crystal diffractometer (a) and simulated from corresponding scXRD data (b).

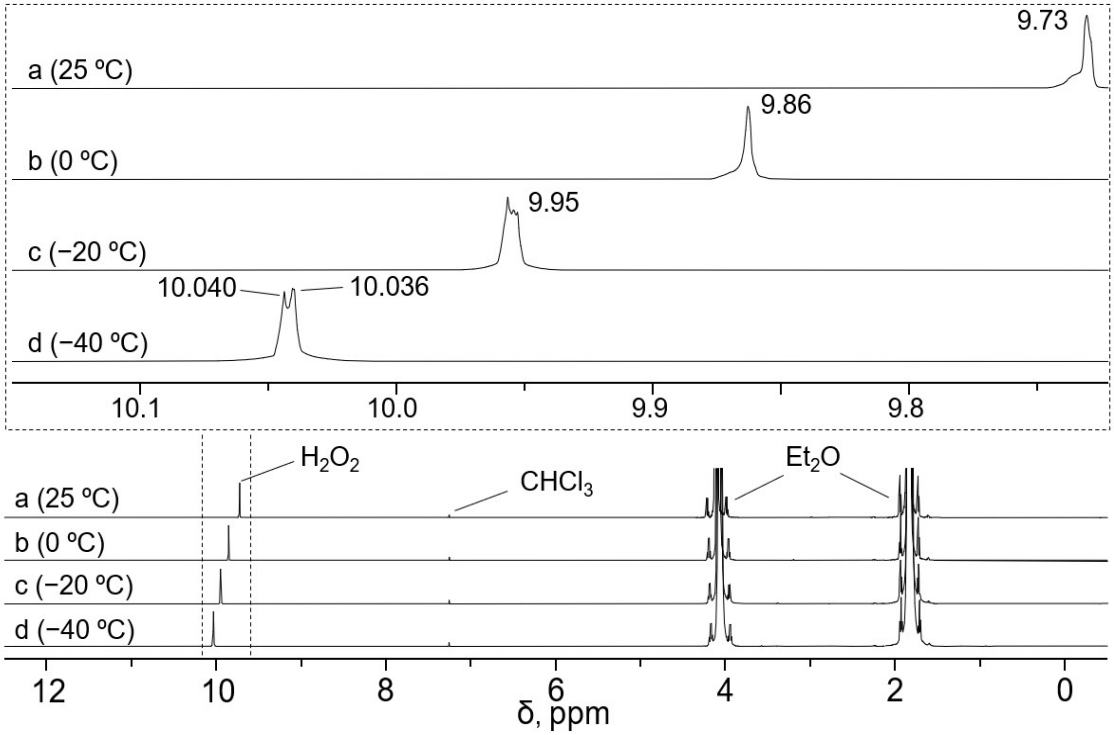

Figure S17. Variable temperature ^{1}H NMR spectra of H_2O_2 in Et_2O (0.03 M) at: a) 25 ºC b) 0 ºC; c) -20 ºC; d) -40 ºC.

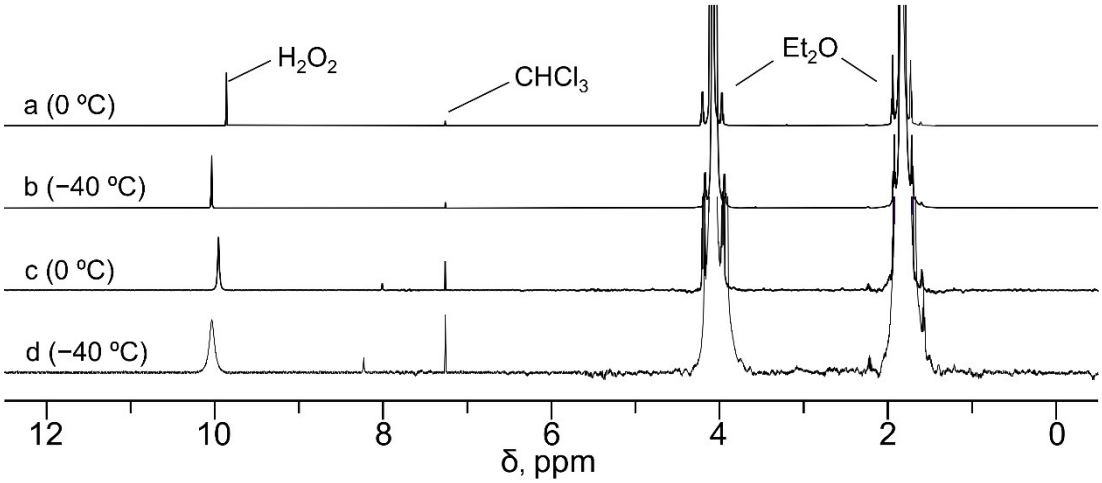

Figure S18. Variable temperature ^{1}H NMR spectra of H_2O_2 in Et_2O (0.03 M) at 0 ºC (a), −40 ºC (b) and its equimolar mixture with $InCl_3$ in Et_2O at 0 ºC (c) and −40 ºC (d).

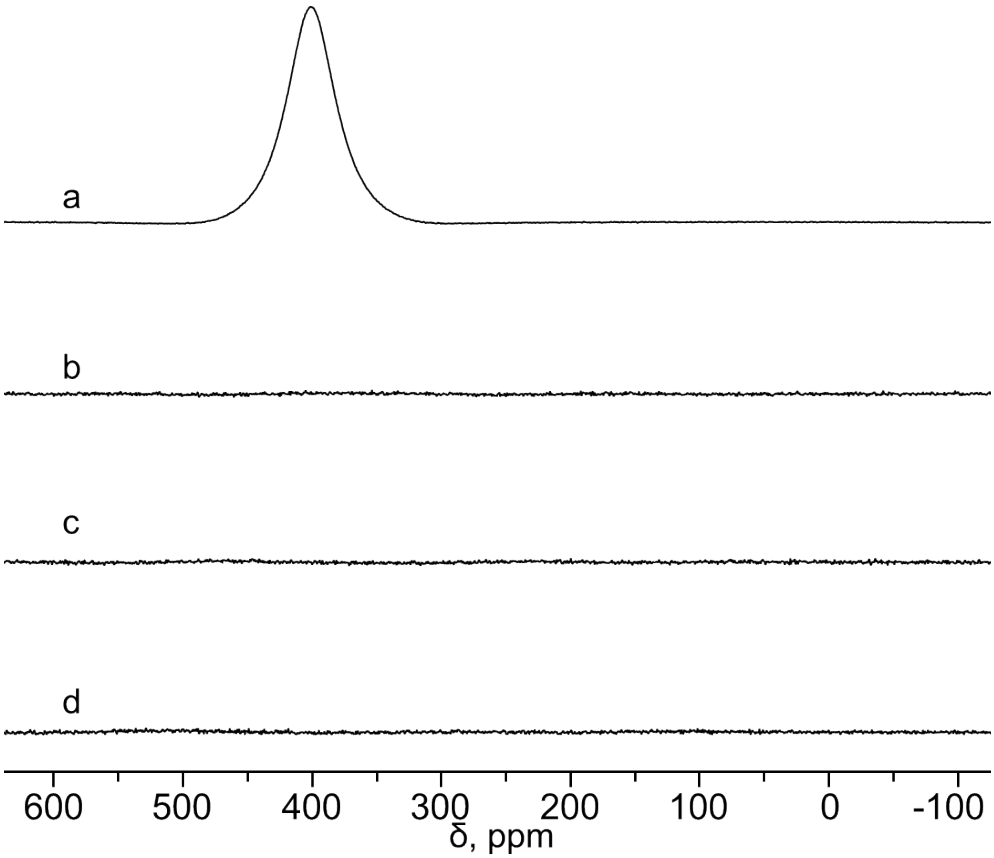

Figure S19. ^{115}In NMR spectra of: a) standard sample containing indium; b) saturated freshly prepared solution of $InCl_3$ and 15-crown-5 (1/2 equiv.) in hydrogen peroxide; c) saturated solution of $InCl_3$ and 15-crown-5 (1/2 equiv.) in hydrogen peroxide, recorded one day after preparation; d) 0.3M of $InCl_3$ in an equimolar mixture of H_2O_2 and Et_2O.

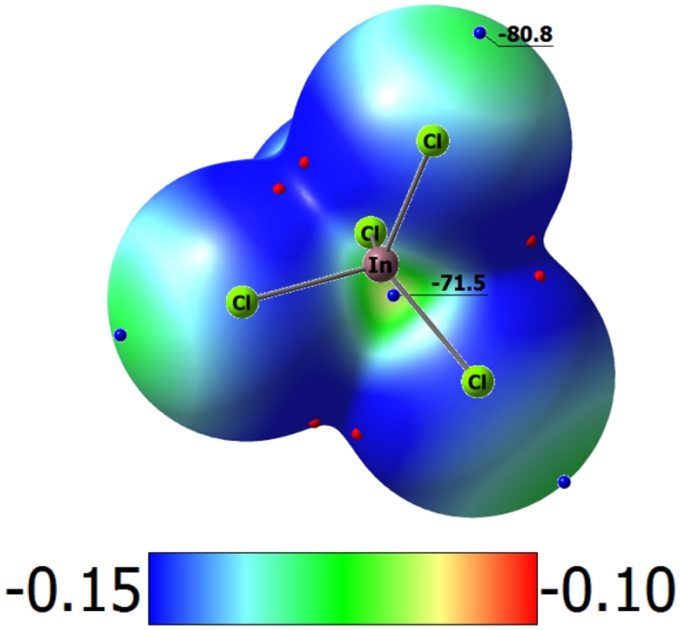

Figure S20. The molecular electrostatic potential (MEP) surface at 0.001 a.u. for $[InCl_4]^-$ anion. MEP maxima ($V_{S,max}$, in kcal/mol) are shown as blue dots, red dots correspond to the MEP minima.

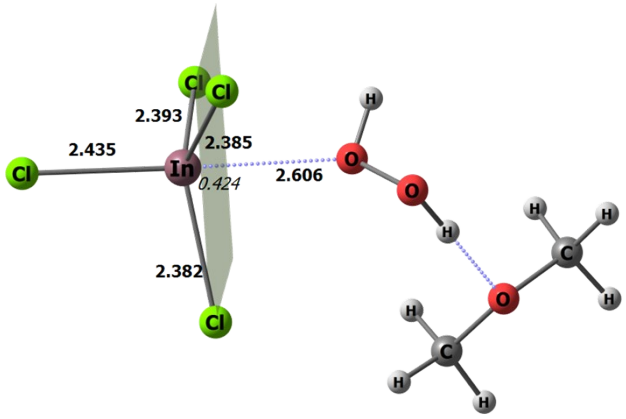

Figure S21. Structures of $[InCl_4]^-$ Lewis adducts with H_2O_2 activated by Me_2O *via* distal OH group, with principal distances (Å). Deviations of the In atom from the Cl_3 plane are in italics. Enthalpy of the complex formation is -2.0 kcal/mol.

3. TABLES

Table S1. Crystal data and details of X-ray analysis of complexes **1**-**5**.

	1	**2**	**3**	**4**	**5**
formula	$C_{10}H_{20}Cl_6In_2O_5$	$C_{12}H_{30}Cl_3In_1O_{10}$	$C_{12}H_{24}Cl_3In_1O_6$	$C_{12}H_{26}Cl_6In_2O_8$	$C_{24}H_{52}Cl_6In_2O_{15}$
*F*w	662.60	555.53	485.48	740.67	1022.99
colour, habit	colourless, prism	colourless, prism	colourless, prism	colourless, prism	colourless, prism
cryst size (mm)	0.10×0.10×0.04	0.10×0.05×0.05	0.10×0.06×0.04	0.10×0.10×0.03	0.15×0.10×0.08
T (K)	100	100	100	100	100
crystal system	monoclinic	triclinic	monoclinic	monoclinic	Orthorhombic
space group	$P2_1$	*P*-1	$P2_1/c$	*Pc*	$Pna2_1$
a (Å)	7.3390(4)	9.2794(3)	21.8566(14)	7.5464(3)	22.8766(7)
b (Å)	19.5292(10)	9.9965(3)	18.1426(11)	11.0757(4)	9.8123(3)
c (Å)	7.3963(4)	13.2310(4)	14.1932(8)	14.9120(6)	8.5596(3)
α (deg)	90	100.777(1)	90	90	90
β (deg)	99.761(2)	90.093(1)	97.734(2)	101.9080(10)	90
γ (deg)	90	117.357(1)	90	90	90
V (Å^3)	1044.73(10)	1065.43(6)	5576.9(6)	1219.55(8)	1921.39(11)
Z	2	2	12	2	2
D_c (g·cm^{-3})	2.106	1.732	1.735	2.017	1.768
μ (mm^{-1})	2.990	1.529	1.724	2.582	1.678
F(000)	640	564	2928	724	1032
θ range (deg)	2.09 to 29.00	2.35 to 25.00	1.46 to 25.00	1.84 to 30.55	2.25 to 30.54
refl collcd	14245	15197	48622	18898	27890
indep reflns / R_{int}	5497 / 0.029	5138 / 0.029	9802 / 0.082	7376 / 0.031	5872 / 0.045
reflns $I>2\sigma(I)$	5223	4716	4347	7170	5285
No of param	230	259	452	261	223
GooF on F^2	1.171	1.031	1.057	1.022	1.027
R_1 ($I>2\sigma(I)$)	0.0298	0.0223	0.0774	0.0223	0.0320
wR_2(all data)	0.0589	0.0464	0.2255	0.0461	0.0542
largest diff peak / hole (e·Å^{-3})	0.82 / -1.02	0.84 / -0.50	1.43 / -1.64	0.57 / -0.90	0.84 / -1.08

CCDC number	**2381797**	**2355318**	**2431051**	**2431052**	**2431053**

Table S2. Selected geometric parameters of **1**-**5**.

	1	**2**	**3**	**4**	**5**
In-O	-	2.4686(14)	-	2.328(3)	2.17(2)
In-O	- -	2.2153(13) 2.1844(13)	-	-	2.284(19)
	2.216(9)- 2.300(9)	-	2.255(7)- 2.321(9)	2.291(2)- 2.347(2)	2.283(3) 2.331(3)
In(1)-Cl In(2)-Cl	2.3899(18) 2.3988(17) 2.3525(19)- 2.3575(16)	2.3849(5)- 2.4233(5) -	2.385(3)- 2.396(4)	2.3689(10) 2.3701(10) 2.3567(10)- 2.4513(10)	2.3943(12)- 2.4132(10)
O(1)-O(2)	-	1.457(2)	-	1.464(4)	1.470(13)
O-In(1)-O	-	75.92(5) 90.55(5) 166.46(5)	70.4(3)- 84.5(4)	68.72(9)- 82.09(8) 137.17(9)- 152.18(8)	70.42(10)- 91.6(6)
O-In(1)-Cl O-In(2)-Cl	83.6 (3)- 96.3(3)	80.76(3)- 100.03(4) 169.33(3)	86.3(3)- 94.6(2) 154.2(2)- 165.2(2)	87.12(7)- 96.39(8) 80.29(7)- 87.47(7) 175.77(7)	86.93(7)-95.1(5) 158.6(4)-163.1(4)

Cl-In(1)-Cl	179.61(7)	98.50(2) 99.36(2) 161.77(2)	98.62(15)- 104.57(12)	178.45(4)	97.20(5)- 104.17(4)
Cl-In(2)-Cl	103.18(7)- 112.30(7)	-		94.16(3)- 123.38(4)	

Table S3. Geometric parameters of hydrogen bonds in the crystal structures of **2**, **4**, and **5**.

D—H···A	D—H, Å	H···A, Å	D···A, Å	∠D—H···A, °
2				
O(1)—H(1)···O(7)	0.85(1)	1.97(1)	2.7916(19)	165(3)
O(3)—H(31)···O(5)	0.83(1)	2.00(1)	2.8342(19)	175(2)
O(3)—H(32)···O(6)^{i}	0.85(1)	2.00(1)	2.8407(18)	176(3)
O(4)—H(42)···O(9)^{ii}	0.84(1)	2.04(1)	2.8359(19)	160(3)
O(4)—H(41)···O(10)	0.84(1)	1.95(1)	2.7785(19)	166(2)
O(2)—H(2)···Cl(2)	0.87(1)	2.33(3)	3.1275(18)	153(5)
Symmetry codes: (i) −*x*+1, −*y*+2, −*z*+1; (ii) −*x*+1, −*y*+1, −*z*				
4				
O(7)—H(7)···O(6)	0.87(4)	1.69(4)	2.557(4)	176(5)
O(8)—H(8)···Cl6^{i}	0.89(4)	2.15(4)	3.033(3)	170(4)
Symmetry code: (i) *x*, −*y*+2, *z*+1/2				
5				
O(1)—H(1)···O(9)	0.80(5)	2.02(4)	2.78(2)	158(5)
O(2)—H(2)···O(7)	0.80(5)	1.80(5)	2.602(7)	176(7)
O(3)—H(3)···O(7)	0.83(5)	2.30(8)	2.97(2)	139(10)
O(3)—H(1)···O(9)	0.82(4)	2.02(4)	2.83(2)	173(5)

Table S4. Complex formation energies (ΔE), enthalpies (ΔH) and Gibbs free energies (ΔG), all in kcal·mol^{-1}; for all discussed complexes.

complex	ΔE	ΔH^{298}	ΔG^{298}
$(H_2O)_2$	-4.4	-2.8	4.2
linear $(H_2O_2)_2$	-4.2	-2.8	4.9
cyclic $(H_2O_2)_2$	-6.2	-4.5	5.3
H-O-H···O_2H_2	-3.2	-1.8	4.8
HO-O-H···OH_2	-5.8	-4.2	3.2
H_2O·imidazole	-6.6	-5.1	2.4
H_2O_2·imidazole	-8.9	-7.5	0.8
HO-O-H···OEt_2	-7.4	-5.7	3.5
HO-O-H···OMe_2	-6.4	-4.9	3.0
O_2H_2···2(OMe_2) [a]	-13.7	-10.5	7.6
H-O-H···OMe_2	-5.1	-3.5	3.7
OH_2···2(OMe_2) [a]	-10.7	-7.4	10.0
HO-O-H···$[InCl_4]^-$	-5.4	-4.1	5.5
H_2O_2···$[InCl_4]^-$	-1.9	-0.6	8.5
$[InCl_4]^-$···O(H)-O-H···$[InCl_4]^-$ [a]	-3.0	-1.8	9.2
Me_2O···H-O-(H)O···$[InCl_4]^-$ [b]	-5.2	-4.0	8.7
2(OMe_2) ···H_2O_2···$[InCl_4]^-$ [c]	-6.1	-4.8	8.0

[a] energies are for trimolecular association

[b] energies are relative to the $[InCl_4]^-$ and HO-O-H···$[InCl_4]^-$ complexes.

[c] energies are relative to the $[InCl_4]^-$ and HO-O-H···OMe_2 complexes.

[d] energies are relative to the $[InCl_4]^-$ and O_2H_2···2(OMe_2) complexes.

Table S5. Cartesian coordinates of optimized structures.

H_2O; E=-76.448402432, H=-76.423000000, G=-76.445066000			
8	0.000000000	0.117354000	0.000000000
1	0.756815000	-0.469414000	0.000000000
1	-0.756815000	-0.469414000	0.000000000
$(H_2O)_2$; E=-152.903858325, H=-152.850531000, G=-152.883507000			
8	1.485419000	0.002894000	-0.116987000
1	1.800009000	-0.019703000	0.786127000
1	0.519032000	0.001647000	-0.043034000
1	-1.748427000	-0.754975000	-0.325497000
8	-1.337860000	-0.002030000	0.101633000
1	-1.751082000	0.766114000	-0.294764000
H_2O_2;E=-151.577876122, H=-151.546560000, G=-151.572942000			
8	-0.703549000	0.104196000	-0.066940000
8	0.703551000	-0.104197000	-0.066937000
1	-1.009500000	-0.580943000	0.535509000
1	1.009481000	0.580953000	0.535502000
$(H_2O_2)_2$ linear; E=-303.162524935, H=-303.097518000, G=-303.138152000			
8	-2.160862000	0.387520000	0.177023000
8	-1.322437000	-0.664599000	-0.290512000
1	-2.276365000	0.158608000	1.103951000
1	-0.446587000	-0.240890000	-0.279004000
8	1.191232000	0.598831000	-0.161670000
8	2.111023000	-0.426975000	0.185635000
1	1.548687000	0.929330000	-0.992584000
1	2.622613000	-0.005272000	0.883832000
$(H_2O_2)_2$ cyclicE=-303.165651639, H=-303.100336000, G=-303.137485000			
8	-1.347818000	0.691626000	-0.114833000
8	-1.485196000	-0.723445000	-0.005641000
1	-1.691026000	0.996225000	0.731547000
1	-0.558894000	-0.988591000	0.120173000
8	1.349009000	-0.691510000	0.116107000
8	1.484305000	0.723660000	0.003921000
1	1.690667000	-0.997122000	-0.730528000
1	0.556847000	0.986831000	-0.117622000
H_2O_2*H_2O Hp-Ow; E=-228.035516173, H=-227.976274000, G=-228.012844000			
8	1.480252000	-0.498927000	-0.105908000
8	0.754563000	0.722792000	-0.003061000
1	1.737862000	-0.660271000	0.806321000
1	-0.171160000	0.409018000	0.000031000
8	-1.842813000	-0.208884000	0.019390000
1	-2.387048000	0.175720000	0.707976000

1	-2.315669000	-0.044314000	-0.797694000
$H_2O*H_2O_2$ Hw-Op;W-PE=-228.031431893, H=-227.972358000, G=-228.010334000			
1	-2.324073000	-0.425397000	0.765347000
8	-2.078478000	-0.115815000	-0.106035000
1	-1.152612000	0.145495000	-0.022194000
8	0.705385000	0.635261000	0.132707000
8	1.417094000	-0.568486000	-0.120439000
1	1.032499000	1.220314000	-0.558569000
1	2.092178000	-0.548101000	0.565557000
Me_2O; E=-155.043884490, H=-154.958519000, G=-154.989166000			
8	-0.000001000	-0.589642000	-0.000007000
6	-1.166484000	0.194883000	0.000000000
1	-2.020643000	-0.479477000	-0.000265000
1	-1.215952000	0.834591000	-0.889026000
1	-1.216164000	0.834162000	0.889317000
6	1.166484000	0.194882000	-0.000001000
1	2.020639000	-0.479484000	0.000043000
1	1.216030000	0.834381000	0.889166000
1	1.216101000	0.834374000	-0.889175000
$H_2O_2*Me_2O$; E=-306.632035586, H=-306.512843000, G=-306.557273000			
8	-2.379844000	0.281862000	-0.327434000
8	-1.677131000	-0.758617000	0.347314000
1	-2.572626000	0.894152000	0.388541000
1	-0.747474000	-0.536579000	0.134594000
8	0.871956000	-0.014898000	-0.286281000
6	1.922743000	-0.927065000	-0.042958000
1	1.603493000	-1.899450000	-0.410670000
1	2.141340000	-0.997240000	1.027034000
1	2.829454000	-0.619673000	-0.571630000
6	1.165365000	1.291514000	0.164683000
1	0.300915000	1.913661000	-0.055444000
1	2.041540000	1.690740000	-0.353996000
1	1.354859000	1.300919000	1.242430000
$H_2O_2*2(Me_2O)$; E=-461.687463034, H=-461.480271000, G=-461.539227000			
8	-0.336268000	-2.079907000	-0.540987000
8	0.536506000	-2.020534000	0.587741000
1	-0.957549000	-1.353024000	-0.345283000
1	1.135653000	-1.292152000	0.333299000
8	2.001037000	0.146306000	-0.259661000
6	2.503070000	1.020805000	0.728599000
1	2.987707000	0.413159000	1.489250000
1	1.695173000	1.598842000	1.188130000
1	3.233040000	1.712236000	0.298000000

6	1.338320000	0.826936000	-1.304915000
1	0.969547000	0.077155000	-2.000111000
1	2.025329000	1.502937000	-1.822084000
1	0.492876000	1.406242000	-0.920461000
8	-1.879629000	0.073930000	0.168520000
6	-2.624736000	0.868323000	-0.727532000
6	-1.480236000	0.772005000	1.327553000
1	-2.876849000	0.248555000	-1.584836000
1	-2.040723000	1.730917000	-1.064450000
1	-3.544685000	1.226324000	-0.255947000
1	-0.868912000	0.095734000	1.920057000
1	-2.350670000	1.088144000	1.910079000
1	-0.891616000	1.658159000	1.067227000
H_2O*Me_2O; E=-231.500409575, H=-231.387068000, G=-231.428411000			
8	-2.363859000	0.000030000	-0.042463000
1	-2.497359000	0.003841000	0.904874000
1	-1.400047000	0.000261000	-0.156583000
8	0.416682000	0.000044000	-0.379915000
6	1.029874000	-1.174718000	0.105854000
1	0.487337000	-2.022173000	-0.307052000
1	0.988467000	-1.216756000	1.199046000
1	2.075979000	-1.226006000	-0.210610000
6	1.031184000	1.174258000	0.105621000
1	0.488980000	2.022194000	-0.306717000
1	2.077085000	1.224727000	-0.211629000
1	0.990620000	1.216081000	1.198846000
$H_2O*2(Me_2O)$; E=-386.553245324, H=-386.351906000, G=-386.407487000			
8	-0.227989000	-2.085284000	-0.448848000
1	0.516378000	-1.470916000	-0.377424000
1	-0.992768000	-1.543469000	-0.212004000
8	-2.176321000	-0.136000000	0.274574000
6	-2.309586000	0.688721000	-0.862959000
1	-2.828566000	0.114041000	-1.626682000
1	-1.328896000	0.992440000	-1.244584000
1	-2.889550000	1.586418000	-0.628214000
6	-1.499854000	0.513523000	1.329136000
1	-1.440764000	-0.184474000	2.161202000
1	-2.038869000	1.411449000	1.645679000
1	-0.485985000	0.796978000	1.026220000
8	1.845256000	-0.182182000	-0.228738000
6	2.467908000	0.085139000	1.007354000
6	1.797192000	0.943547000	-1.075220000
1	2.435821000	-0.829442000	1.595057000

1	1.943720000	0.879930000	1.548752000
1	3.509825000	0.386672000	0.861946000
1	1.288931000	0.644542000	-1.989481000
1	2.805235000	1.292773000	-1.319154000
1	1.243959000	1.765210000	-0.607072000
imidazole; E=-226.240046783, H=-226.163100000, G=-226.193899000			
7	0.136252000	-1.219216000	-0.000110000
6	1.135450000	-0.275780000	0.000099000
6	-0.983730000	-0.535880000	0.000046000
7	-0.753039000	0.794040000	-0.000028000
1	-1.451404000	1.515900000	0.000206000
6	0.602114000	0.979237000	-0.000019000
1	1.048081000	1.957391000	-0.000254000
1	-1.978790000	-0.949537000	0.000087000
1	2.176621000	-0.552989000	0.000166000
H_2O*imidazole; E=-302.698941184, H=-302.594269000, G=-302.635110000			
8	3.182039000	0.000053000	-0.082040000
1	3.448860000	-0.043123000	0.835438000
1	2.203415000	0.006702000	-0.058418000
7	0.356702000	0.016672000	-0.034779000
6	-0.477974000	1.107135000	-0.011803000
6	-0.429204000	-1.034120000	-0.015845000
7	-1.725405000	-0.670415000	0.017902000
1	-2.511981000	-1.294989000	0.037470000
6	-1.776498000	0.696977000	0.020935000
1	-2.705611000	1.236709000	0.045549000
1	-0.111958000	-2.063347000	-0.025143000
1	-0.096055000	2.113871000	-0.020162000
H_2O_2*imidazole; E=-377.832055012, H=-377.721587000, G=-377.765505000			
8	3.034435000	-0.101539000	0.667313000
8	2.530600000	-0.009333000	-0.663516000
1	3.236451000	0.815210000	0.873524000
1	1.549276000	-0.013180000	-0.511969000
7	-0.170381000	0.000337000	-0.232499000
6	-0.975323000	1.103963000	-0.090466000
6	-0.956034000	-1.040358000	-0.080874000
7	-2.224538000	-0.656501000	0.150973000
1	-3.006931000	-1.268823000	0.299917000
6	-2.256983000	0.711635000	0.148664000
1	-3.163865000	1.264557000	0.312387000
1	-0.655722000	-2.073343000	-0.129061000
1	-0.585009000	2.104254000	-0.168434000
Et_2O; E=-233.687121385, H=-233.542295000, G=-233.580196000			

1	-2.377860000	-1.040689000	-0.884842000
8	0.000000000	-0.268390000	-0.000205000
6	1.175431000	0.511500000	0.000163000
6	2.377432000	-0.403975000	-0.000004000
1	1.188167000	1.162364000	0.884117000
1	1.188355000	1.162889000	-0.883403000
1	2.377983000	-1.040122000	-0.885387000
1	3.295216000	0.184016000	0.000332000
1	2.377752000	-1.040737000	0.884936000
6	-1.175431000	0.511501000	-0.000142000
6	-2.377431000	-0.403976000	0.000135000
1	-1.188380000	1.162499000	-0.883996000
1	-1.188147000	1.162754000	0.883525000
1	-2.377872000	-1.040159000	0.885493000
1	-3.295218000	0.184008000	-0.000038000
H_2O_2*Et_2O; E=-385.276816489, H=-385.097915000, G=-385.147625000			
8	-2.187539000	-1.369959000	-0.508455000
8	-1.419163000	-1.334220000	0.690511000
1	-2.877843000	-0.724979000	-0.328158000
1	-0.685901000	-0.734880000	0.441990000
1	-1.496032000	1.717810000	-1.019967000
8	0.576129000	0.376134000	-0.076462000
6	1.939672000	0.001630000	0.026354000
6	2.057827000	-1.493610000	-0.148669000
1	2.329308000	0.311792000	1.002437000
1	2.513177000	0.528793000	-0.743803000
1	1.666981000	-1.800710000	-1.118778000
1	3.104640000	-1.790107000	-0.090219000
1	1.508931000	-2.022210000	0.630818000
6	0.362489000	1.770676000	0.064234000
6	-1.114563000	2.060878000	-0.058155000
1	0.926832000	2.297950000	-0.712540000
1	0.744911000	2.101354000	1.036409000
1	-1.675148000	1.568290000	0.736841000
1	-1.287819000	3.133816000	0.017644000
$InCl_4$; E=-2031.451254860, H=-2031.438166000, G=-2031.483936000			
49	0.000953000	-0.000102000	-0.001161000
17	0.502581000	-2.076451000	1.037529000
17	1.953265000	0.850104000	-1.053301000
17	-1.707499000	-0.318306000	-1.620960000
17	-0.751094000	1.544947000	1.640077000
H_2O_2*$InCl_4$ h-bonded; E=-2183.037787890, H=-2182.991297000, G=-2183.048178000			
8	-3.103968000	0.723156000	-0.078856000

8	-3.512498000	-0.634273000	0.046096000
1	-2.591492000	0.857285000	0.731312000
1	-2.784064000	-1.103760000	-0.388026000
17	-0.669454000	-1.750867000	-1.116896000
49	0.507579000	0.003981000	-0.005664000
17	0.549943000	1.926853000	-1.385074000
17	-0.620770000	0.510337000	2.035271000
17	2.707099000	-0.725127000	0.478249000
H_2O_2*$InCl_4$ In-O; E=-2183.032161500, H=-2182.985713000, G=-2183.043299000			
8	3.336894000	-0.345857000	0.238996000
8	2.384395000	0.530951000	-0.344437000
1	3.939665000	-0.493091000	-0.496898000
1	2.589451000	1.376468000	0.070021000
49	-0.315957000	-0.008228000	-0.004507000
17	-2.712812000	-0.311026000	0.137098000
17	0.327658000	-1.778932000	-1.454212000
17	-0.148476000	2.213276000	-0.858194000
17	0.367894000	-0.238668000	2.263029000
H_2O_2*2($InCl_4$); E=-4214.493756420, H=-4214.432294000, G=-4214.517502000			
8	-0.190900000	2.489625000	0.061118000
8	-0.431451000	1.152721000	-0.341325000
1	0.571147000	2.374441000	0.652056000
1	0.015273000	1.083439000	-1.198504000
49	-2.722840000	-0.083460000	0.004243000
17	-4.723359000	-1.444648000	0.259817000
17	-1.841318000	-0.187936000	2.215222000
17	-1.620336000	-1.281819000	-1.744824000
17	-3.670180000	2.007963000	-0.632784000
17	2.472400000	1.583190000	1.623335000
49	2.889083000	-0.125194000	0.004968000
17	1.759143000	-2.102670000	0.639516000
17	2.176423000	0.623679000	-2.145139000
17	5.226433000	-0.513797000	-0.077685000
Me_2O*H_2O_2*$InCl_4$; E=-2338.091653290, H=-2337.957369000, G=-2338.027271000			
8	-1.299644000	2.469708000	0.459848000
8	-1.182643000	1.302054000	-0.340961000
1	-1.252253000	3.159352000	-0.209219000
1	-2.037380000	0.825693000	-0.165934000
8	-3.437936000	0.040469000	0.135453000
6	-3.306650000	-1.023340000	1.060850000
1	-2.711910000	-0.656759000	1.893988000
1	-2.796471000	-1.873757000	0.599968000
1	-4.290075000	-1.338588000	1.418183000

6	-4.158136000	-0.326862000	-1.026044000
1	-4.189472000	0.542521000	-1.678424000
1	-5.177008000	-0.622366000	-0.763761000
1	-3.662241000	-1.153201000	-1.542635000
49	0.847570000	-0.059422000	-0.030069000
17	2.827120000	-1.499776000	0.070290000
17	1.894492000	1.911536000	-0.890892000
17	-0.482730000	-1.421879000	-1.491033000
17	0.275023000	-0.070344000	2.292675000
$2(Me_2O)*H_2O_2*InCl_4$; E=-2493.148490730, H=-2492.926115000, G=-2493.010368000			
8	1.666876000	-0.412252000	1.522569000
8	1.098805000	0.068257000	0.311756000
1	2.366189000	-0.999651000	1.161930000
1	1.405170000	1.010488000	0.270223000
8	1.954280000	2.557733000	0.188592000
6	0.971426000	3.530890000	0.490548000
1	0.476992000	3.218379000	1.407179000
1	0.233385000	3.595621000	-0.313908000
1	1.437247000	4.508656000	0.636670000
6	2.646738000	2.830739000	-1.014777000
1	3.355964000	2.021607000	-1.172876000
1	3.186233000	3.778007000	-0.937211000
1	1.952515000	2.876348000	-1.858391000
8	3.560286000	-1.900280000	0.299609000
6	4.825782000	-1.272373000	0.278135000
6	3.110271000	-2.265990000	-0.990786000
1	5.084725000	-1.021446000	1.304119000
1	4.798711000	-0.358531000	-0.323363000
1	5.582892000	-1.946066000	-0.132571000
1	2.118548000	-2.697734000	-0.878351000
1	3.786044000	-3.000515000	-1.437694000
1	3.048437000	-1.389888000	-1.643279000
49	-1.274775000	-0.230320000	-0.015800000
17	-3.655175000	-0.477386000	-0.577364000
17	-0.725513000	-2.559010000	0.074521000
17	-0.652825000	1.066175000	-1.943001000
17	-1.550979000	0.925701000	2.065422000

Table S6. FTIR bands' assignment

Compound	Wavenumber, cm^{-1}	Assignment	Reference
H_2O_2	3305 s, br	ν(O–H)	20-22
	2800 w, br	$\nu_2+\nu_6$ in –OOH	20-22
	1326 w, br	δ(H–O–O)	20-22
	880	ν(O–O)	20-22
[*mer*-$InCl_3(H_2O_2)(H_2O)_2$]·18-crown-6 (complex **2**)	Wavenumber, cm^{-1}	Assignment	Reference
	3320 s, br	ν(O–H)	3, 23, 24
	3226 s, shoulder type	ν(O–H) in H_2O	3, 23, 24
	2927−2836 w, br	ν_s(C–H)/ν_{as}(C–H)in CH_2	25
	1620 w, br	δ(H–O–H)	23, 24
	1473 w, br	δ(CH_2)	25
	1354 w, sh	δ(CH_2)	25
	1299 w, br	δ(CH_2)	25
	1257 w, br	δ(CH_2)	25
	1136 w, sh	ν(C–O), ν(C–C)	25
	1087 s, sh	ν(C–O), δ(CH_2)	25
	950 s, sh	δ(CH_2)	25
	835, w, sh	ν(C–O)	25
[*mer*-$InCl_3(H_2O)_3$]·18-crown-6	Wavenumber, cm^{-1}	Assignment	Reference
	3331 s, br	ν(O–H)	3, 23, 24
	3207 s	ν(O–H) in H_2O	3, 23, 24

	2931−2838 w, br	ν_s(C–H)/ν_{as}(C–H)in CH_2	25
	1619 w, br	δ(H–O–H)	23, 24
	1477 w, br	δ(CH_2)	25
	1353 w, sh	δ(CH_2)	25
	1300 w, br	δ(CH_2)	25
	1257 w, br	δ(CH_2)	25
	1136 w, sh	ν(C–O), ν(C–C)	25
	1090 s, sh	ν(C–O), δ(CH_2)	25
	954 s, sh	δ(CH_2)	25
	836, w, sh	ν(C–O)	25
18-Crown-6	Wavenumber, cm^{-1}	Assignment	Reference
	2946−2844 s, sh	ν_s(C–H)/ν_{as}(C–H)in CH_2	25
	1493-1444 w, sh	δ(CH_2)	25
	1355 w, sh	δ(CH_2)	25
	1332 w, sh	δ(CH_2)	25
	1294 w, sh	δ(CH_2)	25
	1258 w, sh	δ(CH_2)	25
	1124 s, sh	ν(C–O), δ(CH_2)	25
	1105 s, sh	ν(C–O), δ(CH_2)	25
	1056 m, sh	ν(C–O)	25
	990 m, sh	δ(CH_2), ν(C–C), δ(CH_2)	25
	944 m, sh	δ(CH_2)	25

	886 w, br	ν(C–O), δ(CH_2)	25
	859 m, sh	ν(C–O), δ(CH_2)	25
	827 w, sh	ν(C–O)	25

4. REFERENCES

1 W. C. Schumb, C. N. Satterfield and R. L. Wentworth, *Hydrogen peroxide*, Reinhold Publishing Corporation, New York, 1955.

2 A. A. Mikhaylov, A. G. Medvedev, P. A. Egorov, N. S. Mayorov, K. Y. Zhizhin and P. V. Prikhodchenko, *Russ. J. Gen. Chem.*, 2024, **94**, 3333–3339.

3 A. B. Ilykhin, Zh. V. Dobrokhotova and S. P. Petrosyants, *Russ. J. of Coord. Chem.*, 2008, **34**, 641–646.

4 L.B. McCusker, R.B. Von Dreele, D.E. Cox, D. Louër, P. Scardi, J. Appl. Crystallogr., *1999*, **32**, №1, 36-50.

5 G. M. Sheldrick, *SADABS ver. 2016/2 - Bruker AXS area detector scaling and absorption correction program*, 2016, Bruker AXS, Karlsruhe, Germany.

6 G. M. Sheldrick, *Acta Crystallogr. C Struct. Chem.*, 2015, **71**, 3–8.

7 B. R. Mcgarvey, C. O. Trudell, D. G. Tuck and L. Victoriano, *Inorg. Chem.*, 2002, **19**, 3432–3436.

8 A. Fratiello, D. D. Davis, S. Peak and R. E. Schuster, *Inorg. Chem.*, 2002, **10**, 1627–1632.

9 T. H. Cannon and R. E. Richards, *Transactions of the Faraday Society*, 1966, **62**, 1378–1387.

10 M. J. Frisch, et al., Gaussian 09, Revision D.01, 2009, DOI: 10.1159/000348293.

11 J. Da Chai and M. Head-Gordon, *Phys. Chem. Chem. Phys.*, 2008, **10**, 6615–6620.

12 D. Kumar Deb and B. Sarkar, *Phys. Chem. Chem. Phys.* , 2017, **19**, 2466–2478.

13 S. Pal, T. K. Kundu, J. G. Han, T. Kar and A. M. Koster, *Int. Sch. Res. Notices*, 2013, **2013**, 753139.

14 F. Weigend and R. Ahlrichs, *Phys. Chem. Chem. Phys.* , 2005, **7**, 3297–3305.

15 M. Mathew, R. Puchta and R. Thomas, *Comput. Theor. Chem.*, 2024, **1233**, 114477.

16 B. Metz, H. Stoll and M. Dolg, *J. Chem. Phys.*, 2000, **113**, 2563–2569.

17 V. Barone and M. Cossi, *J. Phys. Chem. A*, 1998, **102**, 1995–2001.

18 M. Cossi, N. Rega, G. Scalmani and V. Barone, *J. Comput. Chem.*, 2003, **24**, 669–681.

19 T. Lu, *J. Chem. Phys.* **2024**, *161* (8), DOI:10.1063/5.0216272/3309709.

20. J. L. Arnau, P. A. Giguère, M. Abe and R. C. Taylor, *Spectrochim. Acta, Part A*, 1974, **30**, 777–796.

21. R. L. Redington, W. B. Olson and P. C. Cross, *J. Chem. Phys.*, 1962, **36**, 1311–1326.

22. M. Pettersson, S. Tuominen and M. Räsänen, *J. Phys. Chem. A*, 1997, **101**, 1166–1171
23. John E. Bertie, M. Khalique Ahmed and Hans H. Eysel, *J. Phys. Chem.*, 1989, **93**, 2210–2218.
24. J.-B. Brubach, A. Mermet, A. Filabozzi, A. Gerschel and P. Roy, *J. Chem. Phys.*, 2005, **122**, 184509.
25. H. Matsuura, K. Fukuhara and Y. Masuda, *J. Polym. Sci., Part B: Polym. Phys.*, 1986, **24**, 1383–1400.